International Journal of Engineering Trends and Technology
ISSN: 2231 – 5381 /doi:10.14445/22315381/IJETT-V69I12P211
Volume 69 Issue 12, 92-102, December, 2021

Rough Set and Otsu Approach based Hybrid Image Classification under Uneven Lighting Conditions

Mamata Wagh[1], Pradipta Kumar Nanda[2]

[1]*Research scholar, Department of Computer Science and Engineering, SOA University, Bhubaneswar, India*

[2]*Professor, Department of Electronics and Communication Engineering, SOA University, Bhubaneswar, India*

[1]mamtacse7@gmail.com, [2]pknanda@soa.ac.in

***Abstract* —** *Uneven lighting creates vagueness in pixel intensities of the real-world images. This poses a great challenge in the process of image classification. Further, image classification is the fundamental step in the robot vision system. In order to handle the vagueness created due to uneven lighting conditions, a Rough set and Otsu approach-based Hybrid (RSOH) image segmentation scheme is proposed in this research work. In the proposed RSOH scheme, the Otsu and rough set approaches are hybridized in such a way that the resultant hybridized scheme overcomes the limitations of the rough set and Otsu approach and makes use of advantages of both the approaches. Hence, RSOHmodel has the potential to give accurate image classification performance. Through the window growing approach, the image is partitioned into different sub-images, i. e., windows, and inside each window, the proposed RSOHimage segmentation scheme is employed to make the thresholding adaptive. The proposed scheme is compared with granular computing as well as non-granular techniques. The performance of the proposed technique is quantified using four performance indexes such as PM, DC, VI, and BHD. From the performance indexes, it is evident that the proposed RSOH scheme is found to be superior to the existing techniques.*

Keywords — *Image segmentation, Uneven lighting conditions, Adaptive windowing, Granular computing, Rough set, Otsu thresholding.*

I. INTRODUCTION

Classifying an image into different meaningful partitions is a fundamental computer vision task [1, 2, 3]. In this regard, extraction of an object in a given image is a subtle issue while building a computer vision system [4, 5, 6, 7]. Further, in the real world, illumination is uneven and non-linear because of changing environmental conditions [8]. Due to varying illumination over the image, pixel intensity changes suddenly, which leads to a complex background. Further, because of varying illumination, the real-world images are unevenly lighted, and it poses a major challenge in classifying such images in computer vision systems. Image segmentation using thresholding is a popular technique to classify the image into object and background [9]. Thresholding approaches are broadly divided into two types: global and local thresholding. The global thresholding [6] approach can be a suitable choice for evenly illuminated images which are comparatively less complicated to classify because of uniform illumination. However, the global thresholding approach has limitations in handling-uniformly illuminated images [8]. On the other hand, the local thresholding [7, 10] approach makes the threshold for classification adaptive, and hence it is an efficient approach to classify non-uniformly illuminated images.

Besides this, the Otsu method of thresholding was proposed by Otsu [11], which is considered a landmark thresholding method. In today's era also, the Otsu method is extensively studied, and innovative modifications are proposed by researchers [12, 13, 14, 15, 16, 17, 18]. But Otsu method alone is not sufficient to handle the unevenly lighted images because of its limitations. In this regard, hybridization of the Otsu method with other techniques is required for accurate classification.

Because of non-uniform and uncontrolled illumination, uncertainty gets added to the image. Granular computing-based rough sets are the potential tool to handle uncertain, vague, and imprecise data [19]. In granular computing-based rough sets, the information granule is the information entity using which various rough set models are constructed [5, 20, 21, 22]. In real-world images, because of varying illumination, the boundary of an object is rough or vague. In this context, Pawlak's rough set theory [19] is used to extract this rough boundary [5] and shape approximation of an object [23].

The poor visibility conditions encountered due to uneven lighting makes the task of identifying the boundary of an object difficult because of poor boundary information. To handle this issue, a rough set and Otsu-based hybrid (RSOH) image segmentation technique is proposed in this work. The motivation of the proposed scheme is elaborated as follows.

Though the Otsu approach is a landmark approach of thresholding, it has two lacunas. The first lacuna is that the Otsu approach works well with a bi-modal histogram. In the case of images with uneven lighting conditions, due to uncertainty, the histogram can not be bi-modal which is the major reason that the Otsu method can not produce accurate classification in such images. Another lacuna of the Otsu approach is that it works well when the modes of the histogram do not vary much in size. In images with uneven lighting conditions, the modes of the image histogram may vary in terms of size due to uncertainty.

Because of the above two lacunas, the Otsu method alone is not sufficient to classify the images with uneven lighting conditions. Further, though a rough set is a potential tool to handle the uncertainty, its classification performance is influenced by the granule size chosen. In this regard,

attempts are done in literature to fuzzyfy the granules [4, 8, 23]. But, fuzzyfying the granules adds computational complexity and manual tuning of fuzzy constants. This motivated us to hybridize the rough sets and Otsu approach. In the proposed RSOH technique, a rough set is used to get the set of boundary granules. The statistical information of boundary granules has a bi-modal histogram, and also, the modes of the histogram are almost equal in size. Therefore, Otsu computation on the boundary granules instead of the complete window of the image gives an accurate threshold for classification. As the threshold for classification is computed by using Otsumethod, the performance of the proposed RSOH scheme does not depend on the granule size chosen to perform the rough set computation. The proposed RSOH scheme removes the lacunas of the rough set and Otsu approach and makes use of advantages of both the approaches; hence the resultant proposed hybridized model has the potential to give accurate image classification performance.

The proposed technique is tested on standard images from the Berkeley image database. The performance is validated on single as well as multiple object images. To quantify the classification performance of the proposed RSOH technique, the different performance indices (mentioned in Section VI) are evaluated. Based on the computation of said performance indices, it is found that the proposed RSOH technique gives superior classification accuracy compared to the existing techniques.

II. LITERATURE REVIEW

A brief literature review is presented in Table I, in which merits and demerits of existing schemes are highlighted.

TABLE I

LITERATURE REVIEW

Category	Major considerations	Refer-nces
Segmentation	• Classification using different tools and techniques • No specific focus on unevenly illuminated images	[5, 24, 25, 26, 27, 28, 29, 30]
Thresholding	• Efficient schemes are developed to determine the optimum threshold for image segmentation • No specific focus on unevenly illuminated images	[5, 31, 32, 33]
Rough Set	• Mathematical foundation of the rough set is explored, and elegant approaches are proposed for image segmentation •Segmentation performance is dependent on the size of the granule	[5, 4, 23]
Fuzzy granulation	• Fuzzy granulation is proposed to minimize the boundary uncertainty • Fuzzy constants needed to generate fuzzy granules are required to be manually tuned • Fuzzy system increase the computational complexity	[8, 23]
Otsu	• Different novel schemes based on Otsu theory and its generalizations are presented • No specific focus on unevenly illuminated images	[12, 13, 14, 15, 16, 17, 18]

III. PRELIMINARY BACKGROUND

A. Adaptive Windowing

In unevenly illuminated images, due to uneven lighting conditions, illumination varies over the image, and as a result of this, the different portions of the image exhibits different characteristics of data. Therefore, an adaptive windowing approach is used to divide the image into different windows. In this study, the window growing approach is used for adaptive windowing and is elaborated as follows.

In this approach, the entropy criterion is used to fix the windows, and thus the whole image is divided into distinct size windows. Every window (sub-image) is treated separately, and inside each window, the classification of the window as an object and background is performed. The pictorial representation illustrating the window growing approach is shown in Fig. 1.

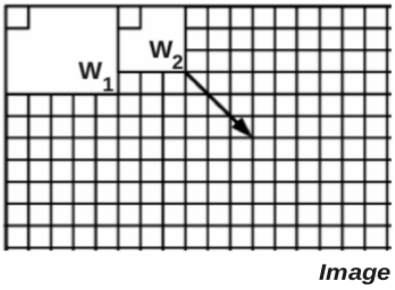

Fig. 1 Adaptive windowing using window growing approach

Referring to Fig. 1, initially, a small window is considered from the upper left corner of the image and is grown with small increments till the entropy criterion is satisfied. Once the entropy criterion is satisfied, the window is fixed, and the next window begins from the adjacent white block, as depicted in Fig. 1. The detailed explanation is as follows.

In the beginning, a small size window 'w_i' is chosen from the upper left corner, and its entropy 'E_w' is computed as

$$E_w = -\sum_{w_i} Pr_{w_i} \log(Pr_{w_i}) \qquad (1)$$

where Pr_{wi} indicates the probability of *with* gray value over the window.
For a complete image, the entropy is computed as,

$$E_I = -\sum_i Pr_i \log(Pr_i) \quad (2)$$

where Pr_i Indicates the probability of the i^{th} gray value.
Window size is fixed if the criterion given below is fulfilled.

$$E_w \geq K.E_I \quad (3)$$

where $K \in [0,1]$ and is a constant. If the initial window considered does not satisfy the entropy criteria given by (3), the size of the window is incremented with Δw, and this procedure is repeated till the entropy criterion is satisfied. The entropy criterion given by (3) ensures the existence of sufficient information or, in other words, the presence of object and background both for classification inside the window. Further, considering each window as a sub-image, the classification is carried out, and the above procedure is repeated till the complete image is covered.

B. Basic Theory of Rough Set

The rough set approximation of set *X* is represented in Fig. 2. As seen from Fig. 2, the positive granules are defined as the granules that are fully interior to set *X* and are illustrated by dark gray shade. The negative granules are defined as the granules that are fully outlier to set *X* and are illustrated by white shade. Further, the granules that are partially interior to set *X* or partially outlier to set *X* are called boundary granules. These boundary granules are illustrated by light gray shade.

The mathematical modeling of rough set theory is given by Pawlak [19] and is elaborated as follows.

Let, information system is $I_{sys} = (U_n, A_t)$, where U_n is the nonempty and finite set of samples $x_1, x_2, x_3, \ldots, x_n$ called as the universe and A_t is a set of attributes. For a subset *X* belongs to U_n, the lower and upper approximation of *X* with respect to U_n is defined as

$$\underline{apr}(X) = \{x \mid x \in U_n, [x] \subseteq X\} \quad (4)$$

$$\overline{apr}(X) = \{x \mid x \in U_n, [x] \cap X \neq \emptyset\} \quad (5)$$

Using the above lower and upper approximation of *X*, the universe U_n gets partitioned into three disjoint regions, and these regions are; (i) the positive region *POS*(*X*) is the union of all granules that are completely included in *X*, (ii) the negative region *NEG*(*X*) is the union of all granules that are excluded from *X*, and (iii) the boundary region *BND*(*X*) is the difference between the upper and lower approximations. These are given as follows:

$$POS(X) = \underline{apr}(X) \quad (6)$$

$$NEG(X) = U_n - POS(X) \cup BND(X) \quad (7)$$

$$BND(X) = \overline{apr}(X) - \underline{apr}(X) \quad (8)$$

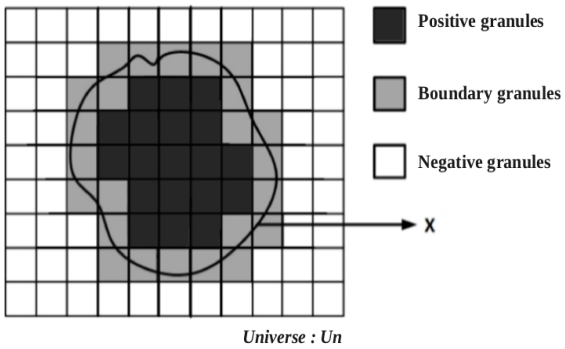

Fig.2: Rough set framework of set X

IV. OVERVIEW OF THE PROPOSED SCHEME

The overall architecture of the proposed scheme is depicted in Fig. 3. Referring to Fig. 3, the image is divided into adaptive windows, and each window of an image is considered as a sub-image. Further, each window is divided into fix size granules. Using these information granules, the rough set model is applied, and lower and upper approximation sets are found. Following this, the set of boundary granules is found out from lower and upper approximations. The probability of intensity values comprised in boundary granules is taken into consideration, and Otsu thresholding is applied to this statistical information to get the optimal threshold. Further, the optimal threshold found is used inside each window to perform the classification of the window into object and background. The process is repeated till all the windows are exhausted, and the union of all the classified windows is the final classified image.

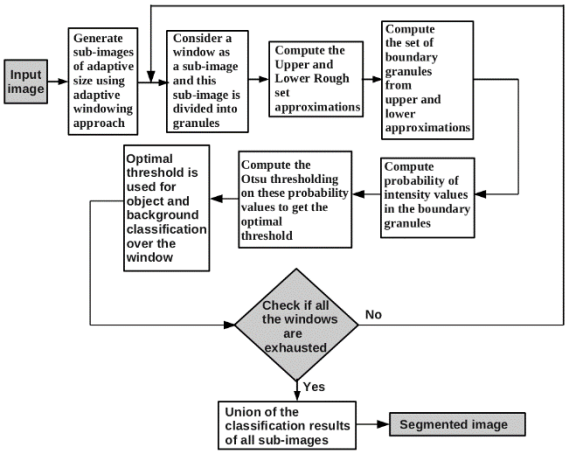

Fig. 3: Overview of the proposed classification scheme

V. PROPOSED ROUGH SET AND OTSUAPPROACHBASEDHYBRID (RSOH) SCHEME

In this Section, Rough Set and Otsu-based Hybrid (RSOH) image classification scheme is proposed and elaborated as follows.

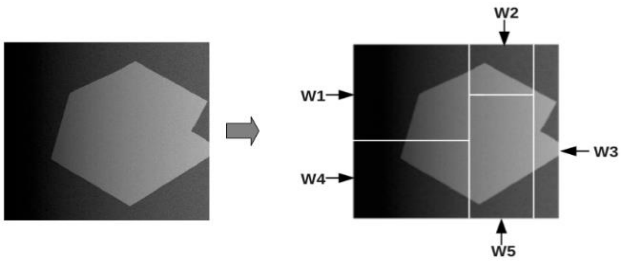

Fig. 4: Generation of adaptive windows over the image

In this scheme, the initial image is divided into different non-overlapping adaptive windows as illustrated in Fig. 4, using the entropy criteria as described in Section III-A. The entropy criterion given by (3) ensures the presence of both objects as well as a background in a given window. Further, every window of the image is divided into granules, as shown in Fig 5. Consider, window W1 of Fig. 4 and corresponding granulation over W1 are shown in Fig. 5.

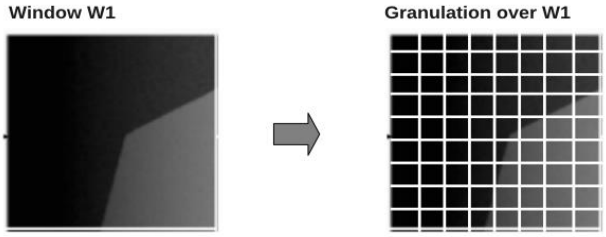

Fig. 5: Granulation over window W1

Using these granules, the lower and upper approximation of the target set is evaluated using (9), (10), (11), and (12), respectively, and the process is elaborated as follows. Let *Gr*ırepresent gray levels. From these total gray levels, the object of an image is represented by 0, ..., *Tr*and background of the image is represented by *Tr*, ..., *Gr*ı-1. Using this framework, the lower and upper approximations of an object, as well as background in the window, is determined as follows.

$$\underline{O}_{w_L} = \{\bigcup_i Gn_i \mid P_j > T, \forall j = 1, \ldots, xy \text{ and } P_j \text{ is a pixel belonging to } Gn_i\} \quad (9)$$

$$\overline{O}_{w_L} = \{\bigcup_i Gn_i, \exists j,\ j = 1, \ldots., xy\ s.t.\ P_j > T, \text{ where } P_j \text{ is a pixel in } Gn_i\} \quad (10)$$

$$\underline{B}_{w_L} = \{\bigcup_i Gn_i \mid P_j \leq T, \forall j = 1, \ldots, xy \text{ and } P_j \text{ is a pixel belonging to } Gn_i\} \quad (11)$$

$$\overline{B}_{w_L} = \{\bigcup_i Gn_i, \exists j, j = 1, \ldots, xy\ s.t.\ P_j \leq T, \text{ where } P_j \text{ is a pixel in } Gn_i\} \quad (12)$$

where, $\underline{O}_{w_L}$ denote the lower approximation of an object, $\overline{O}_{w_L}$ denote the upper approximation of an object, $\underline{B}_{w_L}$ denote the lower approximation of the background, $\overline{B}_{w_L}$ denote the upper approximation of the background and Gn_i Denotes the granule.

From the lower and upper approximations, the boundary granules for object and background are determined as follows.

$$BND^{O}_{Gr} = \overline{O}_{w_L} - \underline{O}_{w_L} \quad (13)$$

$$BND^{B}_{Gr} = \overline{B}_{w_L} - \underline{B}_{w_L} \quad (14)$$

These boundary granules are the elements in the boundary set, and they comprise uncertain data. Moreover, this set of boundary granules possesses a piece of vital information for classification because it is comprised of converged information of different classes.

From the above upper and lower approximations, the roughness index of an object and background over the window is calculated as follows,

$$R^{ind}_{O_{w_L}} = 1 - \frac{|\underline{O}_{w_L}|}{|\overline{O}_{w_L}|} = \frac{|\overline{O}_{w_L}| - |\underline{O}_{w_L}|}{|\overline{O}_{w_L}|} \quad (15)$$

$$R^{ind}_{B_{w_L}} = 1 - \frac{|\underline{B}_{w_L}|}{|\overline{B}_{w_L}|} = \frac{|\overline{B}_{w_L}| - |\underline{B}_{w_L}|}{|\overline{B}_{w_L}|} \quad (16)$$

where$|\cdot|$ indicates cardinality of the set, $R^{ind}_{O_{w_L}}$ defines roughness of the object and $R^{ind}_{B_{w_L}}$ Defines the roughness of the background in the window under consideration.

The total roughness index can be determined from (15) and (16) as follows,

$$R^{ind}_{w} = \left(R^{ind}_{O_{w_L}} + R^{ind}_{B_{w_L}}\right)/2 \quad (17)$$

Further, in the rough set framework, the roughness index is a measure of roughness or vagueness. Hence, to measure the uncertainty, the roughness index is evaluated using the above equations. The minimum roughness index indicates the minimum uncertainty or vagueness. Therefore, minimum roughness or vagueness assures a higher accuracy of classification. In this regard, the roughness index is minimized as follows.

$$R^{ind}_{min} = \arg\min_{Th_w} R^{ind}_{w} \quad (18)$$

The boundary granules at minimum roughness index are collected, and Otsu computation is evaluated on the statistical information of these boundary granules. The boundary granules generated by minimizing the above roughness index are shown inFig. 6. These boundary granules possess the converged and reduced information of the distinct classes. The statistical information is constructed using pixel intensity values of these boundary granules. Further, using this statistical information of boundary granules which are obtained using rough set computation, Otsu computations are performed as follows.

Fig. 6: Set of boundary granules generated by Rough set computation

Let, the pixels of boundary granules of the window has L_w^B distinct intensity levels [0, ..., L_w^B]. The total number of pixels in the set of boundary granules is N_w^B. Let n_i^B Denote the number of pixels at intensity i. Hence, the total number of pixels are: $N_w^B = n_0^B + n_1^B + n_2^B +$, ……, $n_{L_w^B}^B$. With this representation, the normalized probability distribution is determined as;

$$p_i = \frac{n_i^B}{N_w^B} \; ; \; p_i \geq 0 \; ; \; \sum_{i=0}^{L_w^B} p_i = 1 \qquad (19)$$

The pixels of boundary granules of the window are divided into two classes, i.e., object and background. Let these classes be denoted as C_1^w and C_2^w Representing object and background or vice versa. These classes are decided based on the threshold level K_w^B. With this framework, the class C_1^w comprised of pixels in the intensity range [0, ..., K_w^B] and the class C_2^w comprised of pixels in the intensity range [K_w^B +1, ..., L_w^B]. Based on this threshold, the probability of occurrence of class C_1^w As follows.

$$P_1(K_w^B) = \sum_{i=0}^{K_w^B} p_i \qquad (20)$$

On a similar line, the probability of occurrence of class C_2^w It is determined as follows.

$$P_2(K_w^B) = \sum_{i=K_w^B+1}^{L_w^B-1} p_i = 1 - P_1(K_w^B) \qquad (21)$$

The mean intensity level of class C_1^w and C_2^w are determined as;

$$\mu_1 = 1/P_1(K_w^B) \sum_{i=0}^{K_w^B} ip_i \qquad (22)$$

$$\mu_2 = 1/P_2(K_w^B) \sum_{i=K_w^B+1}^{L_w^B-1} ip_i \qquad (23)$$

where, μ_1 is the mean of class C_1^w and μ_2 is the mean of class C_2^w Over the window.

Cumulative mean up to level K_w^B is determined as

$$\mu_k = \sum_{i=0}^{K_w^B} ip_i \qquad (24)$$

and the global mean is determined as,

$$\mu_G = \sum_{i=0}^{K_w^B} ip_i \qquad (25)$$

Based on the above means and probability of occurrence of both the classes, the variance between the two classes are determined as follows,

$$\sigma_v^2(K_w^B) = [\mu_G P_1(K_w^B) - \mu K]^2 / P_1(K_w^B)[1 - P_1(K_w^B)] \qquad (26)$$

The optimum threshold for classification is determined by maximizing the variance between the two classes as follows.

$$\sigma_v^2\left(K_w^{B^*}\right) = \max_{0 \leq K_w^B \leq L_w^B - 1} \sigma_v^2(K_w^B) \qquad (27)$$

The above optimum threshold K_w^B is considered for classifying the window into object and background.

As Otsu computation is performed on the converged and a reduced set of pixel intensity information gained from boundary granules, it leads to better accuracy of classification. Moreover, Otsu computation on this converged information leads to accurate classification as compared to the Otsu computation on the whole window. Thus, the proposed RSOH technique gives the accurate threshold for classifying the window into object and background. On similar lines, all the windows generated by the window growing technique described in Section III-A are classified. The union of all such classified windows is the final classified output image.

The algorithm for the proposed image classification scheme is given below.

Algorithm : RSOH Classification Scheme for image classification.

Input : $Img_{(M \times N)}$: Original image of size M x N.
Δ_w : Fix window increment.
K_c : Positive constant in the range of 0 to 1.
Output : Optimum threshold and a classified image.

Initialize parameters of the algorithm.
for i = 0 to M_f x N_f **do**
  $H_{Img} = -\sum_i P_i \; log(P_i)$ // Entropy of the whole image.
end for
// Adaptive windowing
for $Img_{(conv)}$ = 0 to M_f x N_f **do** // Parent for loop.
  for w = Δ_w to M_w x N_w **do**
    $H_{wind} = -\sum_{wi} P_{wi} \; log(P_{wi})$ // Entropy of the window.
    if ($H_{wind} \geq K_c \times H_{Img}$)
      EXIT // Fix the window size and exit the for loop.
    end if
    else
      $w = w + \Delta w$ // Increment the window size by fix increment.
    end else
  end for
for each window w // window for loop.
  for i = 0 to Gl_w
    $\underline{O}_{w_L} = \{Set \; of \; granules \; which \; are \; completely \; interior \; to \; target \; set \; for \; object\}$,
    $\overline{O}_{w_L} = \{Set \; of \; granules \; which \; are \; completely \; or \; partially \; interior \; to \; target \; set \; for \; object\}$,
    $\underline{B}_{w_L} = \{Set \; of \; granules \; which \; are \; completely \; interior \; to \; target \; set \; for \; background\}$,
    $\overline{B}_{w_L} = \{Set \; of \; granules \; which \; are \; completely \; or \; partially \; interior \; to \; target \; set \; for \; background\}$,
    $BND_{Gr}^O = \overline{O}_{w_L} - \underline{O}_{w_L}$; $BND_{Gr}^B = \overline{B}_{w_L} - \underline{B}_{w_L}$
    $R_{O_{w_L}}^{ind} = 1 - \frac{|\underline{O}_{w_L}|}{|\overline{O}_{w_L}|} = \frac{|\overline{O}_{w_L}| - |\underline{O}_{w_L}|}{|\overline{O}_{w_L}|}$; $R_{\overline{B}_{w_L}}^{ind} = 1 - \frac{|\underline{B}_{w_L}|}{|\overline{B}_{w_L}|} = \frac{|\overline{B}_{w_L}| - |\underline{B}_{w_L}|}{|\overline{B}_{w_L}|}$
    $R_w^{ind} = (R_{O_{w_L}}^{ind} + R_{\overline{B}_{w_L}}^{ind})/2$
    $BND_{Gr} = BND_{Gr}$ *at minimum* R_w^{ind}
  for all the pixel intensities in BND_{Gr} do
    $p_i = n_i^B / N_w^B$; $p_i \geq 0$; $\sum_{i=0}^{L_w^B - 1} p_i = 1$
    $P_1(K_w^B) = \sum_{i=0}^{K_w^B} p_i$; $P_2(K_w^B) = 1 - P_1(K_w^B)$ // Probability of occurrence of class $C1$ and $C2$
    $\mu_1 = 1/P_1(K_w^B) \sum_{i=0}^{K_w^B} ip_i$; $\mu_2 = 1/P_2(K_w^B) \sum_{i=K_w^B+1}^{L_w^B - 1} ip_i$ // Means of class $C1$ and $C2$
    $\mu_K = \sum_{i=0}^{K_w^B} ip_i$; $\mu_G = \sum_{i=0}^{K_w^B} ip_i$ // Cumulative mean and global mean
  $\sigma_v^2(K_w^B) = [\mu_G P_1(K_w^B) - \mu K]^2 / P_1(K_w^B)[1 - P_1(K_w^B)]$ //Between-class varience
  $\sigma_v^2(K_w^{B^*}) = \max_{0 \leq K_w^B \leq L_w^B - 1} \sigma_v^2(K_w^B)$ //Maximize the between class variance
  return the optimal threshold, $K_w^{B^*}$ to classify the window.
  end for // End of window for loop.
end for // End of parent for loop.

VI. RESULTS AND DISCUSSIONS

The classification efficiency of the proposed scheme is tested and validated with unevenly lighted images considered from the Berkeley database. Images with both single as well as multiple objects are considered. The classification performance of the proposed scheme has been compared with granular as well as non-granular techniques. The non-granular techniques considered for comparison are Otsu, FCM, and PCM. The granular techniques considered for comparison are Pal's method [5], Heterogeneous Granulation based Window Growing (HGWG) [8], and Empirical Non-homogeneous Granulation based Window Growing (ENHWG) [8]. To validate the quantitative classification performance of the proposed RSOH scheme, different performance indices [34] are used, and these are; (*i*) Percentage of Misclassification (PM), (*ii*) Dice Coefficient (DC), (*iii*) Variance of Information (VI) and (*iv*) Boundary Hamming Distance (BHD).

Index *PM* varies in the range of 0 to 100, and a lower *PM* value indicates higher accuracy. Index DC varies in the range of 0 to 1, and a higher *DC* value indicates higher accuracy. Index *VI* varies in the range of 0 to 1, and a lower *VI* value indicates higher accuracy. Index *BHD* varies in the range of 0 to 1, and a higher *BHD* value indicates higher accuracy.

Further, for every image, different adaptive windows are generated based on entropy criteria, and inside each window, the proposed RSOH scheme is employed to get the optimal threshold for classifying the corresponding window. For example, in the 'hexa' image, the different windows produced and the respective optimal thresholds determined by the proposed RSOH scheme are given in Table II. They considered images are of two categories, i.e., images having a single object as well as images having multiple objects.

A. Category I: Single object images

Images in the single object category are shown in Figs. 7-9. The first image taken into consideration is shown in Fig. 7(a). The corresponding ground-truth and border ground-truth are depicted in Fig. 7(b) and Fig. 7(c), respectively. In this typical image, because of uneven lighting over the image, the poor visibility
condition created over the lower-left region of the mage, which makes the image obscure. Additionally, because of the light falling on the right-wing of the image, there are sharp pixel intensity changes in this region which makes the image difficult to classify. Because of this, the existing techniques have shown considerable misclassification in the said regions of the image, as shown in Figs. 7(d) - 7(i). However, the proposed RSOH scheme could handle the uneven lighting condition, as seen in Fig. 7(j). It can be observed from Table III that *PM* is 1.61% which shows a considerable reduction in misclassification error as compared to the other existing techniques. This effect can be observed from other performance indices given in Tables IV, V, and VI.

Another image tested is the Hexa image presented in Fig. 8(a), and the corresponding ground-truth and border ground-truth is presented in Fig. 8(b) and Fig. 8(c), respectively. It can be observed from Fig. 8(a) that there is evidence of more lighting in the right part of the image, and also, there is the occurrence of poor visibility condition in the lower-left portion of the image. Because of this, the existing techniques failed to classify the image with higher classification error, and it is evident from Figs. 8(d) - 8(i). Moreover, the proposed RSOH scheme could perform accurate classification, and it can be seen from Fig. 8(j). This effect is also reflected by the performance indices given in Tables III, IV, V, and VI.

Let's consider another image of chopper depicted in Fig. 9(a), and corresponding ground-truth and border ground-truth are shown in Fig. 9(b) and Fig. 9(c), respectively. It can be observed from 9(a) that there is the occurrence of complex background because of clouds in the image. Moreover, some intensities of the cloud portion of the image match with the object, i.e., chopper. Because of this, in other classification techniques, a considerable portion of the background is misclassified as an object, and it can be seen from figs. 9(d) - 9(i). The proposed RSOH scheme classification performance leads to accurate classification, which can be seen in Fig. 9(j). This effect is also reflected by the performance indices given in Tables III, IV, V, and VI.

B. Category II: Multiple object images

The images considered in multiple object categories are shown in Figs. 10-12. The first image considered in this category is, grains image shown in Fig. 10. In this typical image, there is evidence of more light in the right upper corner of the image and the poor visibility condition in the lower-left portion of the mage. Because of this, in other classification techniques, many pixels in the right upper corner of the image are misclassified as objects, and many rice grains are misclassified as background, and it can be seen from figs. 10(d) - 10(i). The proposed RSOH scheme could handle this heavily lighted and poor visibility condition arised due to uneven lightings, which can be observed from Fig. 10(j). This effect is also reflected by the performance indices given in Tables VII, VIII, IX, and X.

Another image considered in this category is 'hills and tree', which is depicted in Fig. 11(a). In this image, there is evidence of a complex background because of various layers of hills. It can be seen from Fig. 11(j) that the proposed RSOH classification scheme could perform well as compared to other existing techniques. This effect is evident from Figs. 11(d) - 11(j) and also from the qualitative performance indices given in Tables VII, VIII, IX, and X.

The last image considered in this category is the boat image shown in Fig. 12(a). In this image, there is evidence of sharp intensity changes due to light falling on the water body and the layers of hills in the background. Because of this, other classification techniques have shown a lot of background portion is misclassified as an object, and it can

be observed from Figs. 12(d) - 12(i) . It can be seen from Fig. 12(j) that the proposed RSOH classification scheme could perform well as compared to other existing techniques. This effect is evident from Figs. 12(d) - 12(j) and also from the qualitative performance indices given in Tables VII, VIII, IX, and X.

TABLE II

ADAPTIVE WINDOWS PRODUCED WITH RESPECTIVE THRESHOLDS GIVEN BYRSOHTECHNIQUE IN 'HEXA' IMAGE

Window Number	Window Corners				Threshold $(K_w^{B^*})$
	st-r	st-c	ed-r	ed-c	
1.	0	0	210	210	41
2.	0	210	130	350	69
3.	0	350	400	400	79
4.	210	0	400	210	73
5.	350	210	400	350	37

(st-r: starting row, st-c: starting column, ed-r: ending row, ed-c:ending column.)

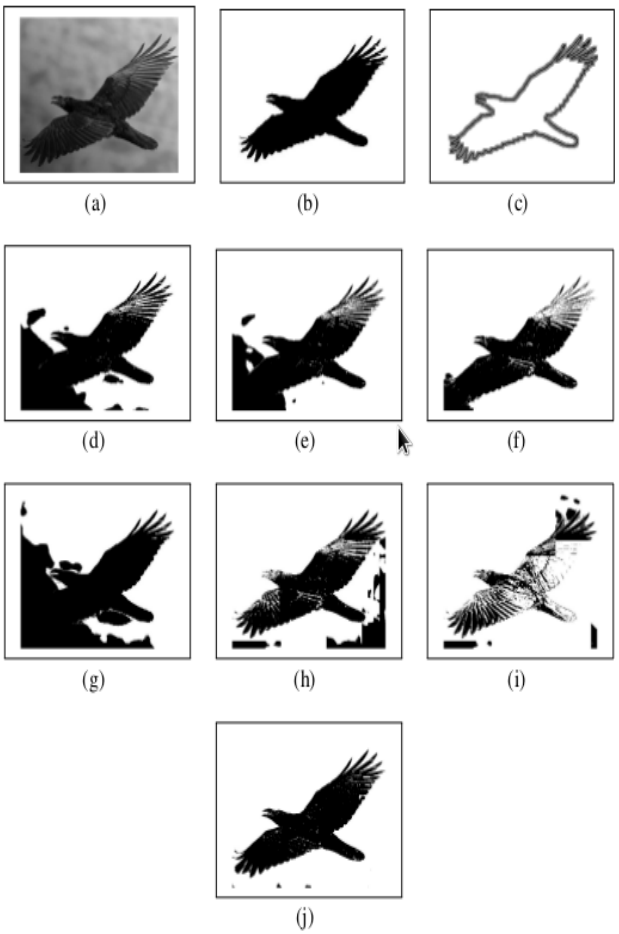

Fig. 7: (a) 'Bird' image (b) Ground-truth (c) Boundary ground-truth (d) Otsu's method (e) Fuzzy C-means (f) Possibilistic C-mean (g) Pal's method (h) Hetero-geneous granulation (HGWG) (i) Non-homogeneous granulation (ENHWG) (j) Proposed RSOH scheme

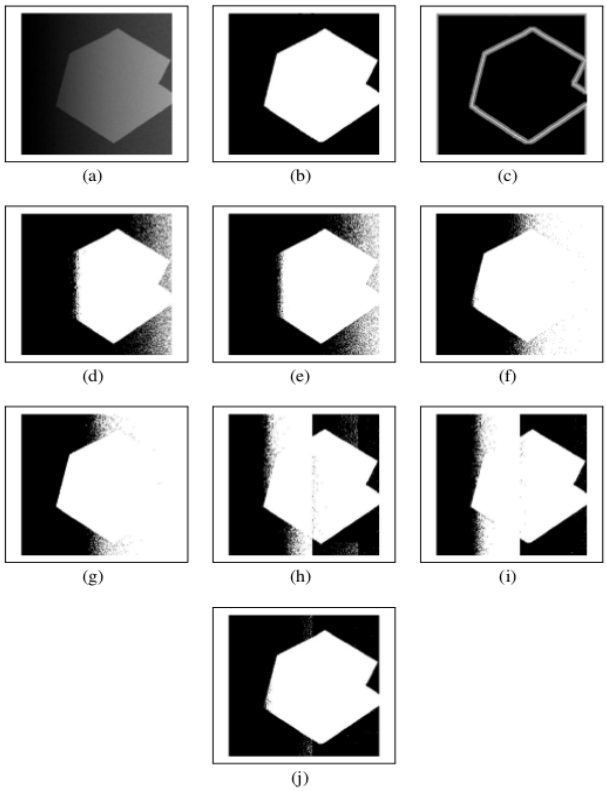

Fig. 8: (a) 'Hexa' image (b) Ground-truth (c) Boundary ground-truth (d) Otsu's method (e) Fuzzy C-means (f) Possibilistic C-mean (g) Pal's method (h) Heterogeneous granulation (HGWG) (i) Non-homogeneous granulation (ENHWG) (j) Proposed RSOH scheme

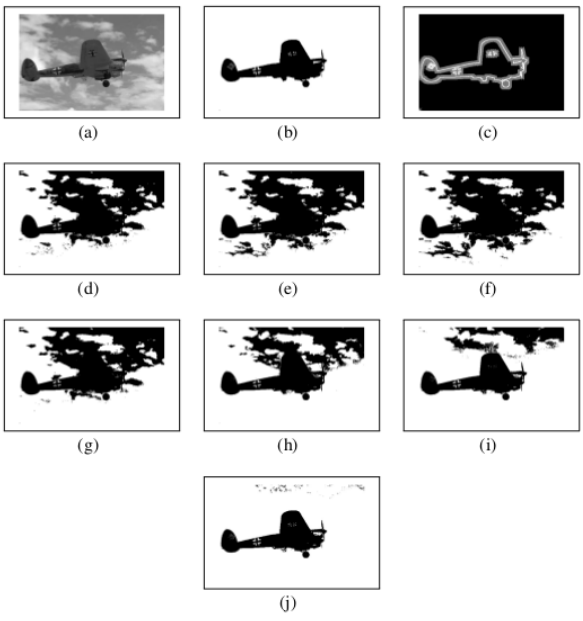

Fig. 9: (a) 'Chopper' image (b) Ground-truth (c) Boundary ground-truth (d) Otsu's method (e) Fuzzy C-means (f) Possibilistic C-mean (g) Pal's method (h) Heterogeneous granulation (HGWG) (i) Non-

homogeneous granulation (ENHWG) (j) Proposed RSOH scheme.

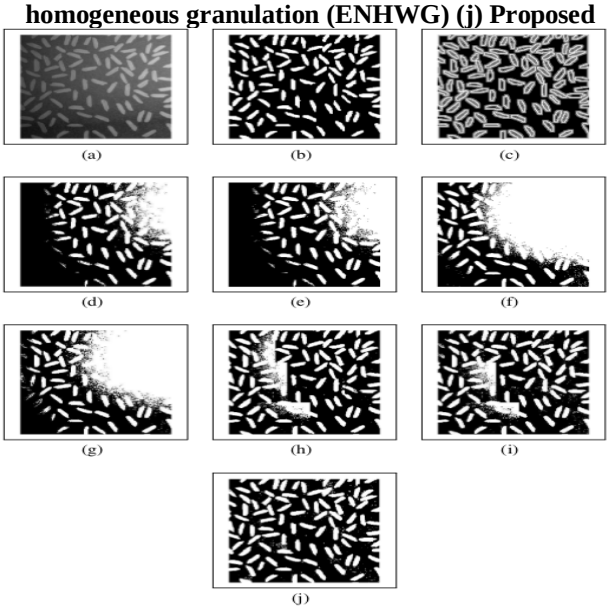

Fig. 10. (a) 'grains' image (b) Ground-truth (c) Boundary ground-truth (d) Otsu's method (e) Fuzzy C-means (f) Possibilistic C-mean (g) Pal's method (h) Hetero-geneous granulation (HGWG) (i) Non-homogeneous granulation (ENHWG) (j) Proposed RSOH scheme

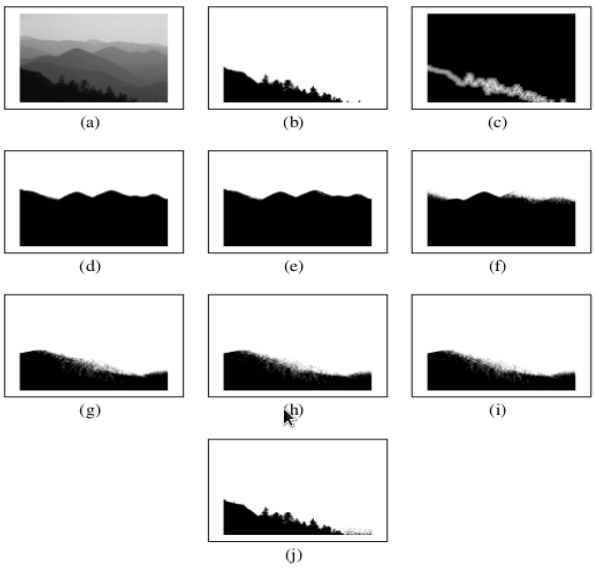

Fig. 11. (a) 'Hills and tree' image (b) Ground-truth (c) Boundary ground-truth (d) Otsu's method (e) Fuzzy C-means (f) Possibilistic C-mean (g) Pal's method (h) Heterogeneous granulation (HGWG) (i) Non-homogeneous granulation (ENHWG) (j) Proposed RSOH scheme

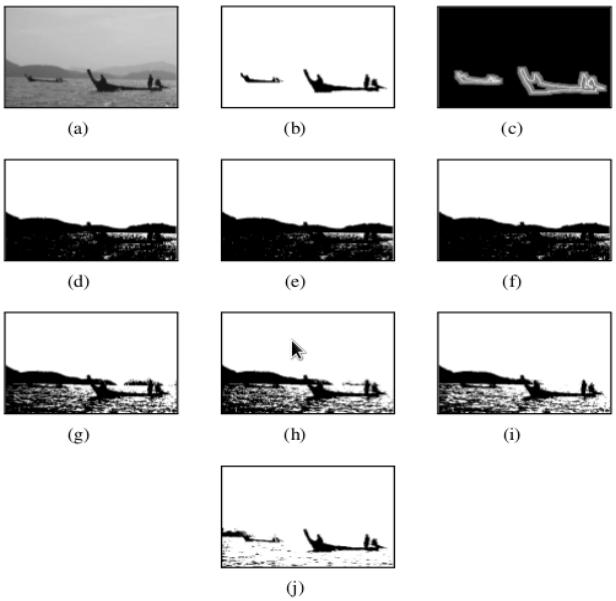

Fig. 12. (a) 'Boat' image (b) Ground-truth (c) Boundary ground-truth (d) Otsu's method (e) Fuzzy C-means (f) Possibilistic C-mean (g) Pal's method (h) Hetero-geneous granulation (HGWG) (i) Non-homogeneous granulation (ENHWG) (j) Proposed RSOH scheme

To estimate the robustness of the proposed RSOH scheme, the detailed comparative analysis of the Average Classification Performance (ACP) of various schemes using index PM is given in Table XI. ACP is calculated by taking the average of PM for all images. It is evident from Table XI that the proposed RSOH scheme is more robust as compared to the existing techniques.

TABLE III

CLASSIFICATION PERFORMANCE USING INDEX PM FOR IMAGES CONSISTING OF SINGLEOBJECT

Image	Otsu	FCM	PCM	Pal's	HGWG	ENHWG	RSOH
bird	14.37	12.36	11.71	21.03	11.12	17.40	1.61
hexa	10.94	12.49	20.11	20.33	9.90	12.43	1.00
chopper	29.85	32.93	35.56	28.32	21.03	11.82	0.98

TABLE IV

CLASSIFICATION PERFORMANCE USING INDEX DC FOR IMAGES CONSISTING OF SINGLEOBJECT

Image	Otsu	FCM	PCM	Pal's	HGWG	ENHWG	RSOH
bird	0.8562	0.8721	0.8154	0.7897	0.8887	0.8259	0.9857
hexa	0.8905	0.8750	0.7988	0.7968	0.9009	0.8756	0.9901
chopper	0.7015	0.6706	0.6443	0.7167	0.7897	0.8818	0.9971

TABLE V

CLASSIFICATION PERFORMANCE USING INDEX VI FOR IMAGES CONSISTING OF SINGLEOBJECT

Image	Otsu	FCM	PCM	Pal's	HGWG	ENHWG	RSOH
bird	0.3980	0.3284	0.3001	0.4957	0.3477	0.6411	0.1152
hexa	0.3517	0.3859	0.5368	0.5411	0.2860	0.3524	0.0233
chopper	0.5738	0.6168	0.6506	0.5513	0.4337	0.2617	0.0281

TABLE VI

CLASSIFICATION PERFORMANCE USING INDEX BHD FOR IMAGES CONSISTING OF SINGLEOBJECT

Image	Otsu	FCM	PCM	Pal's	HGWG	ENHWG	RSOH
bird	0.8286	0.7523	0.7133	0.7887	0.9157	0.7565	0.9746
hexa	0.8017	0.7829	0.7133	0.7094	0.8722	0.8457	0.9974
chopper	0.8000	0.7653	0.7451	0.8219	0.9196	0.9805	0.9796

TABLE VII

CLASSIFICATION PERFORMANCE USING INDEX PM FOR IMAGES CONSISTING OF MULTIPLE OBJECTS

Image	Otsu	FCM	PCM	Pal's	HGWG	ENHWG	RSOH
grains	20.21	21.46	39.31	32.35	12.47	11.59	8.11
hillstree	41.72	41.56	38.33	12.45	11.15	11.15	1.10
boat	31.59	31.79	32.46	22.90	18.59	15.47	4.51

TABLE VIII

CLASSIFICATION PERFORMANCE USING INDEX DC FOR IMAGES CONSISTING OF MULTIPLEOBJECTS

Image	Otsu	FCM	PCM	Pal's	HGWG	ENHWG	RSOH
grains	0.7980	0.7854	0.6068	0.6764	0.8753	0.8840	0.9187
hillstree	0.5827	0.5843	0.6166	0.8754	0.8883	0.8884	0.9899

boat	0.6840	0.6820	0.6754	0.7709	0.8141	0.8452	0.9589

TABLE IX

CLASSIFICATION PERFORMANCE USING INDEX VI FOR IMAGES CONSISTING OF MULTIPLE OBJECTS

Image	Otsu	FCM	PCM	Pal's	HGWG	ENHWG	RSOH
grains	0.6453	0.6774	0.8419	0.7778	0.3446	0.3235	0.2391
hillstree	0.7296	0.7279	0.6938	0.2746	0.2478	0.2477	0.0299
boat	0.5389	0.5416	0.5499	0.5068	0.3481	0.2957	0.0941

TABLE X

CLASSIFICATION PERFORMANCE USING INDEX BHD FOR IMAGES CONSISTING OF MULTIPLE OBJECTS

Image	Otsu	FCM	PCM	Pal's	HGWG	ENHWG	RSOH
grains	0.7881	0.7762	0.5692	0.6408	0.8783	0.8881	0.9181
hillstree	0.5020	0.5020	0.5020	0.5322	0.5559	0.5559	0.9375
boat	0.4264	0.4201	0.3995	0.5090	0.7307	0.7911	0.9699

TABLE XI

AVERAGECLASSIFICATION PERFORMANCE(ACP) USING INDEX PM

Schemes	Otsu	FCM	PCM	Pal's	HGWG	ENHWG	RSOH
ACP	24.78	25.43	29.58	22.89	14.05	13.31	2.86

VII. CONCLUSIONS

In this work, efforts are made to classify the image accurately into object and background under uneven lighting conditions in the computer vision system. The vagueness and ambiguity caused by uneven lighting conditions are a challenge in classifying such images. In order to deal with this challenge, a hybrid, i. e., a combination of Otsu and rough set (RSOH), is developed.

The proposed scheme is compared with different classification techniques, and to quantify the performance, the four performance indices, i.e., PM, DC, VI, and BHD, are used.

In the proposed work, the two-class problem of classification of unevenly lighted images consisting of single as well as multiple objects is handled. The work presented in this paper will be explored further for multi-class classification.

REFERENCES

[1] Tao Wang, ZexuanJi, Quansen Sun, Qiang Chen, Qi Ge, and Jian Yang, Diffusive likelihood for interactive image segmentation, Pattern Recognition, 79 (2018) 440–451.

[2] A. Bhandary, A. Prabhuand, M. Basthikodi, and K. Chaitra, Early diagnosis of lung cancer using computer-aided detection via lung segmentation approach, International Journal of Engineering Trends and Technology, 69(5) (2021) 85–93.

[3] Weliwita, JAP Isuru, and S. C. Premaratne, Modeling abandoned object detection and recognition in real-time surveillance, International Journal of Engineering Trends and Technology, 69 (2) (2021) 188–193.

[4] D. Chakraborty, B. U. Shankar, and S. K. Pal, Granulation, rough entropy and spatiotemporal moving object detection, Applied Soft Computing, 13(9) (2013) 4001 – 4009.

[5] S. K. Pal, B. U. Shankar, and P. Mitra, Granular computing, rough entropy, and object extraction, Pattern Recognition Letters, 26 (16) (2005) 2509 – 2517.

[6] T. Deng and W. Xie, Granule-view based feature extraction and classification approach to color image segmentation in a manifold space, Neurocomputing, 99 (2013) 46 – 58.

[7] Qingming Huang, Wen Gao, and WenjianCai, Thresholding technique with adaptive window selection for uneven lighting image, Pattern Recognition Letters, Vol. 26(6) (2005) 801–808.

[8] MamataWagh, Pradipta Kumar Nanda, Fuzzy granulation and constraint neighborhood granulation structure for object classification in unevenly illuminated images, Applied Soft Computing, 74 (2019) 306–329.

[9] Qingmao Hu, ZujunHou, and WieslawLucjanNowinski, Supervised range-constrained thresholding, IEEE Transactions on Image Processing, 15(1) (2006) 228–240.

[10] P. Kanungo and P. K. Nanda and A. Ghosh, Parallel genetic algorithm-based adaptive thresholding for image segmentation under uneven lighting conditions, In proceedings of the IEEE International Conference on Systems, Man and Cybernetics, (2010) 1904–1911.

[11] N. Otsu, A threshold selection method from grey-level histogram, IEEE Trans. on Systems, Man and Cybernetics,. 9(1) (1979) 62–66.

[12] EkoPrasetyo, R. Dimas Adityo, NanikSuciati, and ChastineFatichah, Mango leaf image segmentation on hsv and ycbcr color spaces using otsu thresholding,3rdInternational Conference on Science and Technology - Computer (ICST), (2017) 99–103.

[13] Hasnae El Khoukhi, Youssef Filali, Ali Yahyaouy, My AbdelouahedSabri, and AbdellahAarab, A hardware implementation of otsu thresholding method for skin cancer image segmentation, International Conference on Wireless Technologies, Embedded and Intelligent Systems (WITS), (2019) 1–5.

[14] Patil Priyanka Vijay and N. C.Patil, Grayscale image segmentation using otsu thresholding optimal approach, Journal for Research, 2(05) (2016).

[15] Y. Feng, H. Zhao, Li Xiongfeiand X. Zang, A multi-scale 3d otsu thresholding algorithm for medical image segmentation, Digital Signal Processing, 60 (2017) 186–199.

[16] Ashish Kumar Bhandari, Immadisetty Vinod Kumar, and Kankanala Srinivas, Cuttlefish algorithm-based multilevel 3-d otsu function for color image segmentation, IEEE Transactions on Instrumentation and Measurement, 69(5) (2019) 1871-1880.

[17] AmilaAkagic, Emir Buza, Samir Omanovic, and AlmirKarabegovic. Pavement crack detection using otsu thresholding for image segmentation. 5 (2018).

[18] Ta Yang Goh, ShafrizaNishaBasah, HanizaYazid, Muhammad Juhairi Aziz Safar, and FathinulSyahir Ahmad Saad Performance analysis of image thresholding: Otsu technique, Measurement, 114 (2018) 298–307.

[19] Z. Pawlak, Rough Sets: Theoretical Aspects of Reasoning about Data. Theory and Decision Library D: System theory, knowledge engineering, and problem-solving. Springer Netherlands,(2012).

[20] R. Jensen and Qiang Shen, Fuzzy-rough sets for descriptive dimensionality reduction, Proceedings of the IEEE International Conference on Fuzzy Systems (FUZZ-IEEE), 1 (2002) 29–34.

[21] AvatharamGanivada, ShubhraSankar Ray, and Sankar K. Pal, Fuzzy rough granular self-organizing map and fuzzy rough entropy, Theoretical Computer Science, 466 (2012) 37 – 63.

[22] Abdullah Balamash, WitoldPedrycz, Rami Al-Hmouz, and Ali Morfeq, An expansion of fuzzy information granules through successive refinements of their information content and their use to system modeling, Expert Systems with Applications, 42(6) (2015) 2985–2997.

[23] S. K. Pal, S. K. Meher, and S. Dutta, Class-dependent rough fuzzy granular space, dispersion index and classification, Pattern Recognition, 45(7) (2012) 2690 – 2707.

[24] Ricardo L De Queiroz, Zhigang Fan, and Trac D Tran, Optimizing block-thresholding segmentation for multilayer compression of compound images, IEEE Transactions on Image Processing, 9(9) (2000) 1461–1471.

[25] Zizhao Zhang, Fuyong Xing, Xiaoshuang Shi, and Lin Yang, Revisiting graph construction for fast image segmentation Pattern Recognition, 78 (2018) 344–357.

[26] Khai-Yin Lim and RajeswariMandava, segmenting object with ambiguous boundary using information-theoretic rough sets, AEU-International Journal of Electronics and Communications, 77 (2017) 50–56.

[27] B. Wang, L. L. Chen, and M. Wang, Novel image segmentation method based on pcnn, Optik, 187 (2019) 193–197.

[28] Huizhu Pan, WanquanLiu, Ling Li, and Guanglu Zhou, A novel level set approach for image segmentation with landmark constraints, Optik, 182 (2019) 257–268.

[29] Yousheng Wang, XueGao, Yuting Wang, and Jinge Sun, Adventitia segmentation in intravascular ultrasound images based on improved snake algorithm, Optik, 241 (2021) 167-175.

[30] Xiaodong Long and Jian Sun, Image segmentation based on the minimum spanning tree with a novel weight, Optik, 221 (2020) 165308.

[31] A. Verma S. Arora, J. Acharya and P. K. Panigrahi. Multilevel thresholding for image segmentation through a fast statistical recursive algorithm, Pattern Recognition Letters, 29(2) (2008) 119–125.

[32] Zhi-Kai Huang and Kwok-Wing Chau, A new image thresholding method based on gaussian mixture model, Applied Mathematics and Computation, 205(2) (2008) 899–907.

[33] Sunil K. Sinha and Paul W. Fieguth. Segmentation of buried concrete pipe images, Automation in Construction, 15(1) (2006) 47–57.

[34] MiroslavBeneˇs and Barbara Zitova, Performance evaluation of image segmentation algorithms on microscopic image data, Journal of microscopy, 257(1) (2015) 65–85.